A method of texture inhomogeneity estimation from reflection pole figures

1992 J. Phys.: Condens. Matter 4 339

(http://iopscience.iop.org/0953-8984/4/2/003)

J. Phys.: Condens. Matter 4 (1992) 339–349. Printed in the UK

A method of texture inhomogeneity estimation from reflection pole figures

A Morawiec
Instytut Podstaw Metalurgii, Polska Akademia Nauk, ulica W S Reymonta 25, PL 30-059 Krakow, Poland

Received 9 April 1991

Abstract. A method of determining the inhomogeneity of the orientation distribution of crystallites is presented. It makes use of the fact that the reflection pole figures measured by x-ray or neutron diffraction contain information from the whole volume penetrated by the radiation. This allows one to calculate the texture function at different depths in the sample. The results of the calculation tests are given.

1. Introduction

The inhomogeneity of crystallites orientation distribution (texture) in polycrystalline materials is a rule rather than an exception. Frequently it is assumed that it is weak enough to be neglected. Often some restrictions on the deformation process are imposed to minimize texture inhomogeneity.

What we are interested in is the case of a flat sample with its texture changing with depth. The usual way of investigating such an inhomogeneity is by cutting off thin layers (thinning the specimen) repeatedly, measuring the x-ray reflection pole figures and calculating texture function in each step. This method is not only destructive but also cumbersome (see, e.g., Bauer *et al* 1977).

The method described below is based on the fact that reflection pole figures measured by x-ray or neutron diffraction contain information from several layers of the material. The influence of a given layer on the pole figure shape depends on the layer depth. Knowing this dependence quantitatively, one can attempt to calculate from a given set of pole figures not only one (as usually) but two or even more texture functions describing the textures of layers (Morawiec 1990).

It is clear that such a method will be restricted by the fact that the penetration depth is determined by the radiation used. X-rays penetrate only a very thin layer; thus only surface texture can be separated from the interior texture. When based on the neutron pole figure measurements, because of the high penetration depth, inhomogeneities of thick layers can be analysed. If necessary, the neutron penetration can be limited using a non-permeable mask (Choi *et al* 1979).

The difficulties with the standard (i.e. only one) texture function reproduction are the source of doubts about the possibility of getting two or more texture functions from the same set of pole figures. However, the results of tests on models show that from the viewpoint of calculations such a procedure in most cases is admissible.

0953-8984/92/020339 + 11 $04.50

2. Pole figures in terms of the texture function

For the orientation distribution reproduction from pole figures in the case of an inhomogeneous sample it is necessary to know the equation expressing the pole figures by the texture functions in the layers.

Let the function $F(\cdot, x): \mathrm{so}(3) \to \mathbb{R}_+$ describe the orientation distribution in a layer situated at a depth between x and $x + \mathrm{d}x$. The intensity of the reflection with the scattering vector $\boldsymbol{h}$ and $\boldsymbol{y}$ as its direction in the sample coordinate system is given by

$$I_{\boldsymbol{h}}(\boldsymbol{y}) = q(\boldsymbol{h}, \boldsymbol{y}) \int_0^T \mathrm{d}x\, p(\boldsymbol{h}, \boldsymbol{y}, x) \int_{\mathrm{so}(3)} \mathrm{d}g\, F(g, x) \delta(\boldsymbol{h} \pm g\boldsymbol{y}) \qquad |\boldsymbol{y}| = |\boldsymbol{h}| \tag{1}$$

where x equals T for the deepest reflecting level and $q(\boldsymbol{h}, \boldsymbol{y})$ is the coefficient taking into account all intensity corrections not considered explicitly (e.g. defocalization, reflectivity of reflection $\boldsymbol{h}$). Moreover, $p(\boldsymbol{h}, \boldsymbol{y}, x) := s(\boldsymbol{h}, \boldsymbol{y}, x) r(\boldsymbol{h}, \boldsymbol{y}, x)$ where $s(\boldsymbol{h}, \boldsymbol{y}, x)$ is the x-deep surface area from which the radiation can be counted and $r(\boldsymbol{h}, \boldsymbol{y}, x)$ describes the influence of absorption in the material:

$$r(\boldsymbol{h}, \boldsymbol{y}, x) := \Phi_{\boldsymbol{h}}(l(\boldsymbol{h}, \boldsymbol{y}, x)) / \Phi_{\boldsymbol{h}}(0) \tag{2}$$

with $\Phi_{\boldsymbol{h}}(l)$ being the intensity of radiation after a path of length l in the material.

For a homogeneous sample with a random orientation distribution ($F(g, x) = 1$ for all $g \in \mathrm{so}(3)$ and $x \in [0, T]$) the last integral in equation (1) equals 4π. Hence, the $\boldsymbol{h}$ pole figure $P_{\boldsymbol{h}} \propto I_{\boldsymbol{h}} / I_{\boldsymbol{h}}^{\mathrm{random}}$ is given by the expression

$$P_{\boldsymbol{h}}(\boldsymbol{y}) \propto \left(\int_0^T \mathrm{d}x\, p(\boldsymbol{h}, \boldsymbol{y}, x) \right)^{-1} \int_0^T \mathrm{d}x\, p(\boldsymbol{h}, \boldsymbol{y}, x) \int_{\mathrm{so}(3)} \mathrm{d}g\, F(g, x) \delta(\boldsymbol{h} \pm g\boldsymbol{y}). \tag{3}$$

This is the generalized form of the so-called fundamental equation. It takes the standard form

$$P_{\boldsymbol{h}}(\boldsymbol{y}) \propto \int_{\mathrm{so}(3)} \mathrm{d}g\, f(g) \delta(\boldsymbol{h} \pm g\boldsymbol{y}) \tag{4}$$

when the material is homogeneous (i.e. $F(g, x)) = f(g)$).

In the case of an inhomogeneous sample the problem to be solved is to calculate the x-dependent texture function F. The basis for this is equation (3). For a given set of pole figures it represents the system of integral equations.

3. Texture function reproduction

As is known, even in the simplest case of a homogeneous sample the solution of equation (4) is ambiguous. If the texture function f is expanded into a series of generalized spherical harmonics (Fourier series on the rotation group), then the odd part of the series has no influence on the pole figures' shape and therefore can be arbitrarily chosen. On the other hand, the range of the possible solutions is bounded by the non-negativity of the texture function. This formal condition as well as others of physical character allow one in most cases to obtain solutions which can be considered as satisfying equation (4) and the assumed conditions. However, in the case of depth-dependent textures, the information contained in a few pole figures may be too poor to give a satisfactory solution in all its generality, but it can be adequate if additional assumptions are imposed.

To simplify the problem let us assume that the x-dependent texture function can be treated as a superposition of N functions $f^i : \mathrm{so}(3) \to \mathbb{R}_+$:

$$F(g,x) \propto \sum_{i=1}^{N} \xi_i(x) f^i(g). \tag{5}$$

It is assumed that physical reasons allows one to deduce the form of the $\xi_i : \mathbb{R}_+ \to \mathbb{R}_+$ functions and that each of f^i has the properties of a texture function, i.e. it fulfils adequate symmetry conditions.

It should be mentioned here that the symmetry of an inhomogeneous sample cannot be higher than its symmetry when inhomogeneity is neglected. Only the symmetry elements with the rotation axis perpendicular to the plane of constant x cannot be disturbed by inhomogeneity in depth. However, if the layers are considered as homogeneous, the sample symmetry of the texture functions f^i can be higher than the real symmetry of the whole sample.

Equation (3) can now be rewritten as

$$P_h(y) \propto \sum_{i=1}^{N} \rho_i(h,y) \int_{\mathrm{so}(3)} \mathrm{d}g\, f^i(g) \delta(h \pm gy) \tag{6}$$

with

$$\rho_i(h,y) := \left(\int_0^T \mathrm{d}x\, p(h,y,x) \right)^{-1} \int_0^T \mathrm{d}x\, p(h,y,x) \xi_i(x). \tag{7}$$

Thus the problem differs from the standard one (equation (4)) in the number of texture functions to be reproduced.

The principal ambiguity analogous to that of the standard problem occurs also here, i.e. the odd parts of Fourier series of f^i functions do not influence the pole figures, but no other additional ambiguity of a principal character (i.e. occurring for arbitrary pole figures and arbitrary texture functions) does appear. To prove this it is enough to note that from equation (6) it follows that

$$P_h(y) \propto \sum_{i=1}^{N} \rho_i(h,y) P_h^i(y) \tag{8}$$

where P_h^i is the pole figure corresponding to the f^i texture function. If the set of N pole figures of the same type but measured with different Bragg angles, i.e. different ρ_i coefficients (e.g. {200}, {400}, for cubic crystal symmetry) is known, then equation (8) can be considered as a system of N algebraic linear equations for the values of N P_h^i pole figures. Thus the generalized problem can be reduced to the standard one if only the system (8) has an unambiguous solution. This method was applied by Choi *et al* (1979) to the determination of pole figures corresponding to different layers in the sample. However, it is restricted by the difficulties with the measurement of many different pole figures of the same type.

In most of the lately developed methods of solving the standard problem, it is assumed that pole figures and texture functions are piecewise constant and equation (4) is reduced to a system of algebraic linear equations. Besides the principal ambiguity

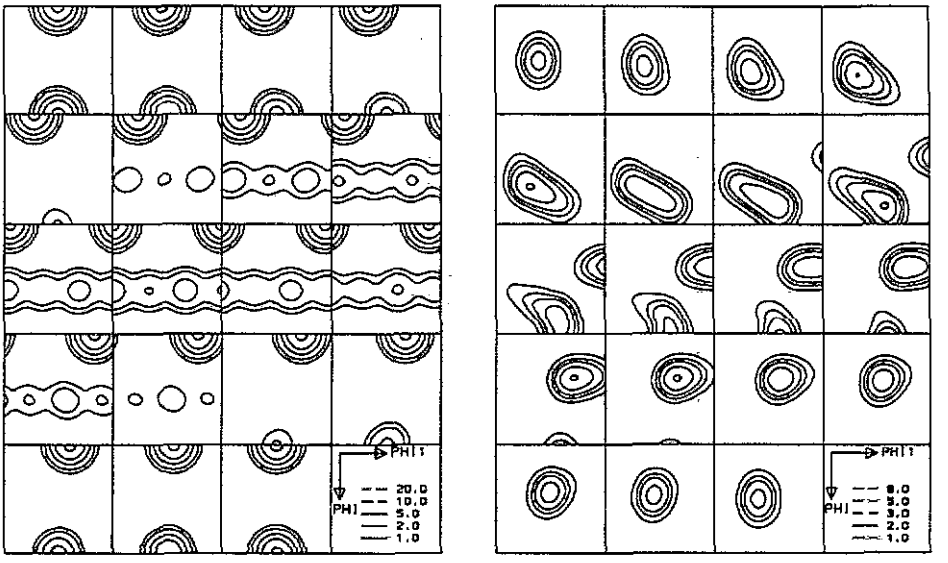

(*a*) (*b*)

Figure 1. Model texture functions: (*a*) function f^1 describing the surface texture; (*b*) function f^2 describing the interior texture.

there may appear another ambiguity resulting from the small number of equations. The non-negativity condition improves the situation, but it makes the problem non-linear and difficult to analyse; therefore, to check the efficiency of the reproduction methods, model calculations are necessary. They show that the results are different in individual cases but sometimes one can obtain a satisfactory solution even from one pole figure (see, e.g., Ruer and Baro 1977, Matthies 1990).

When equation (6) is treated in a similar way, the number of unknowns increases N times and there are doubts about whether a satisfactory solution can be obtained even for $N = 2$. However, in spite of this doubt an appropriate routine has been prepared. In fact, it is a modification of the program solving the standard problem and this in turn is similar to the methods described, for example, by Imhof (1983), Pawlik (1986) and Ruer and Baro (1977). Virtually the routine iteratively solves the system of linear equations built on the basis of equation (6).

4. Tests

The results of some model tests are given below. These tests were carried out on a chosen exemplary texture. It should be emphasized that some graphs can have an individual character, i.e. they can have different shapes for other textures.

The example was chosen to satisfy the most frequently analysed symmetry conditions, i.e. cubic crystal symmetry and orthorhombic symmetry of the layers, and the considered texture functions are well known.

The used coordinates on SO(3) were Euler angles defined according to Bunge (1982). Calculations were carried out with texture functions and pole figures given at grid of 5° mesh size.

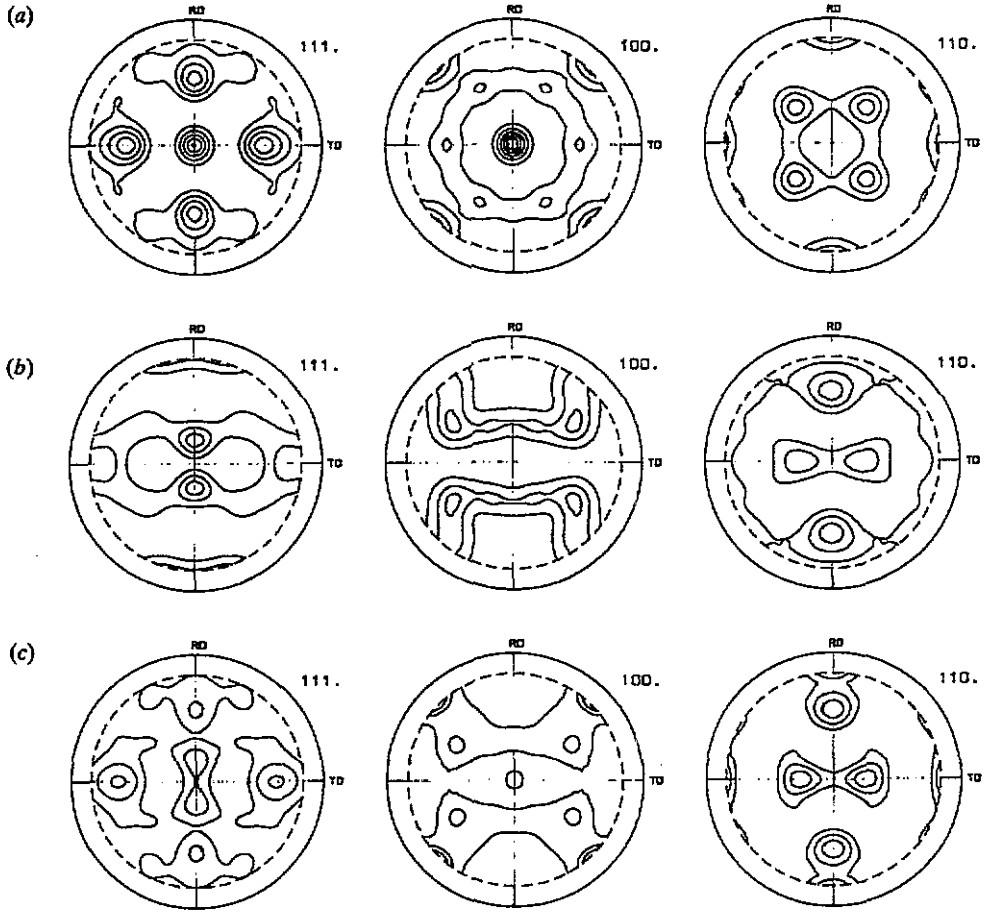

Figure 2. Model pole figures: (*a*) pole figures corresponding to f^1 texture function, obtained using equation (4); (*b*) pole figures corresponding to f^2 texture function, obtained using equation (4); (*c*) pole figures treated as experimental, obtained on the basis of equation (8) following from equation (6).

Except for the non-negativity of the texture function the routine does not contain any other explicitly formulated conditions. Therefore, when using the program, one should be aware of the ambiguity problem.

In the model the assumed texture changes violently at the depth $x = \mathcal{A}$; above and below this level the textures are homogeneous. Equation (5) takes the form

$$F(g, x) \propto H(x)H(\mathcal{A} - x)f^1(g) + H(x - \mathcal{A})f^2(g) \tag{9}$$

where H denotes Heaviside's function. The assumed value of $\mathcal{A}$ is $\mathcal{A}_0 = 1.3 \times 10^{-6}$ m. The functions f^1 and f^2 are taken from the work of Truszkowski *et al* (1979). Each is built of three Gaussian-shaped components (see, e.g., Matthies *et al* 1987). The components and their volume fractions are as follows:

f^1: $\{001\}\langle 110\rangle - 0.46$ $\{111\}\langle 110\rangle - 0.33$ $\{111\}\langle 112\rangle - 0.21$

f^2: $\{110\}\langle 112\rangle - 0.18$ $\{213\}\langle 364\rangle - 0.58$ $\{112\}\langle 111\rangle - 0.24$

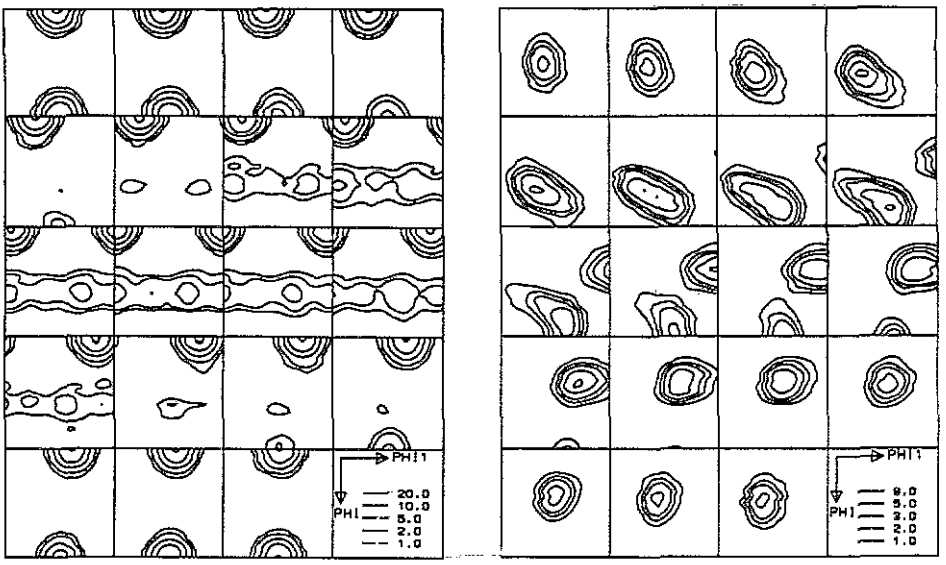

(*a*) (*b*)

Figure 3. Texture functions reproduced from pole figures shown in figure 2(*c*) (after 300 iterations).

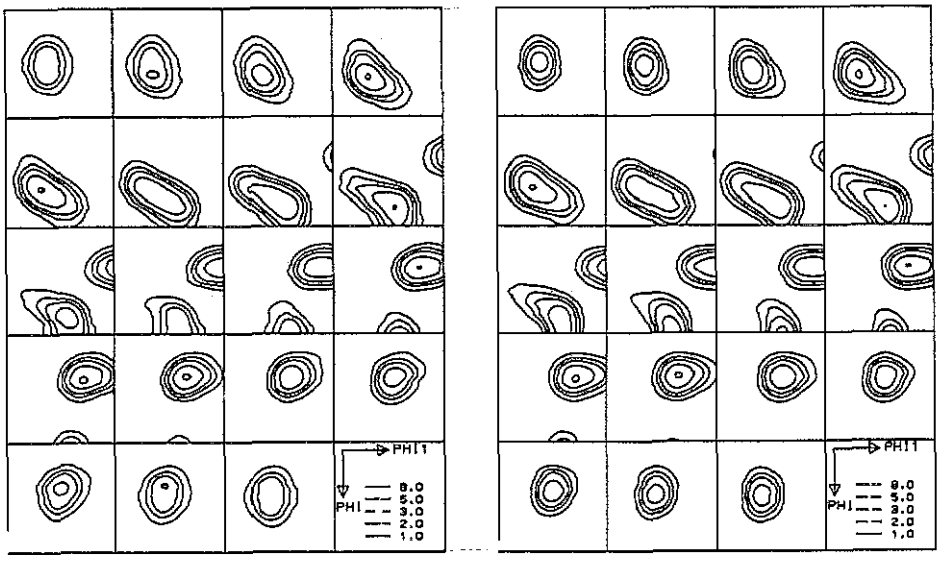

(*a*) (*b*)

Figure 4. Texture functions reproduced from pole figures corresponding to function f^2 (see figure 2(*b*)). Comparison with figure 1(*b*) shows that the method works in case of homogeneous samples. The number of iterations was 300.

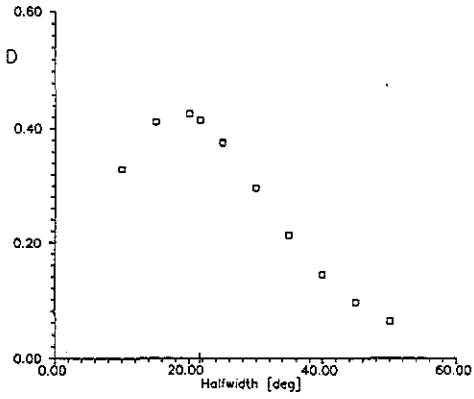

Figure 5. The quality of reproduction versus the sharpness of textures represented by the components half-width after 50 iterations.

All the components (except the test with the results given in figure 5) have the same half-width of 21.6°. The assumed material is copper and the assumed radiation is x-ray copper K_α. The corresponding absorption coefficient is $\mu = 4.7219 \times 10^4\ \mathrm{m}^{-1}$ and the Bragg angles related to the {111}, {100}, {110} and {311} pole figures are 21.67°, 25.24°, 37.09° and 45.00°, respectively. The function s is assumed to be x independent; so it does not influence the ρ^i coefficients. The r-function is defined as $r(\boldsymbol{h}, y, x) = \exp[-\mu l(\boldsymbol{h}, y, x)]$ with

$$l(\boldsymbol{h}, y, x) = 2x/\{\sin[\vartheta(\boldsymbol{h})]\cos[\alpha(y)]\} \tag{10}$$

where ϑ is the Bragg angle and α is the radial angle on a pole figure. Except for the explicitly indicated cases, three pole figures ({111}, {100} and {110} with $\alpha \in [0°, 80°]$ were used.

The idea of the tests is very simple: one considers a given texture (with known texture function) as the really existing texture (figure 1) and then calculates the corresponding pole figures (figure 2). These pole figures are treated as experimental and are the basis for the texture function reproduction. The result can be compared with the assumed texture functions (figures 3 and 4).

Further, the quality of the reproduced texture functions f_c^1 and f_c^2 is characterized by $D := [\mathrm{diff}(f^1, f_c^1) + \mathrm{diff}(f^2, f_c^2)]/2$ with $\mathrm{diff}(f^i, f_c^i) := (8\pi^2)^{-1} \int_{so(3)} \mathrm{d}g\, |f^i(g) - f_c^i(g)|$. This index does not give information on the details but it does show the global difference between the desired 'real' texture and the calculated texture.

In practice, when model texture functions are unknown, the only known quantity characterizing the quality of the texture functions under reproduction is that which describes the differences between the experimental pole figures and the pole figures calculated from these texture functions. A few different quantities of this type are being used. Here the average difference d between the experimental and the calculated pole figures at one measuring point is applied.

It is known that in the standard case the sharpness of the texture affects the quality of the reproduction results. To check this in the generalized case a test was carried out with nine different (but the same for all components) half-widths. As figure 5 shows, the curve has its maximum near the 21.6° point assumed in other tests. The reproduction results for sharper and for flatter textures are better.

Figures 6 and 7 visualize the course of the iteration process. For comparison, analogous curves for one texture function reproduction are shown. The latter have a larger

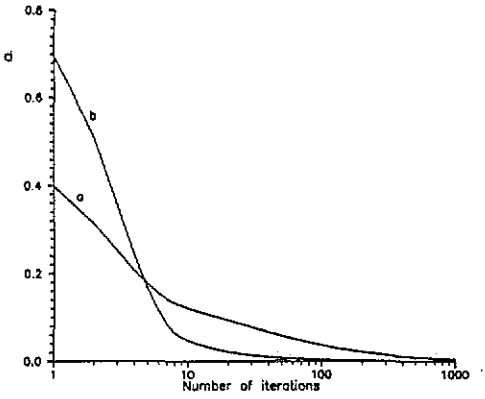

Figure 6. The adjustment of calculated and model pole figures versus number of iterations: (a) case of an inhomogeneous sample: (b) standard case based on equation (4), where the curve represents the arithmetic average for calculations reproducing independently the texture functions f^1 and f^2.

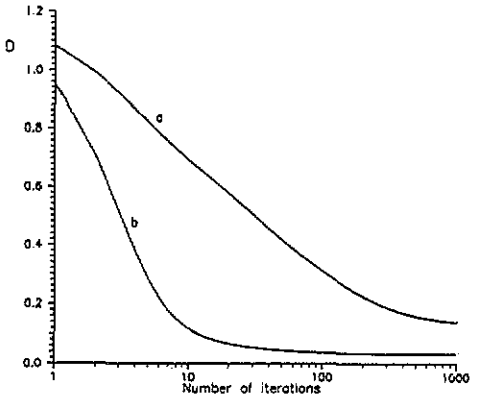

Figure 7. Difference between model and reproduced texture functions versus number of iterations: (a) case of an inhomogeneous sample; (b) curve calculated for functions f^1 and f^2 under separate reproduction according to equation (4).

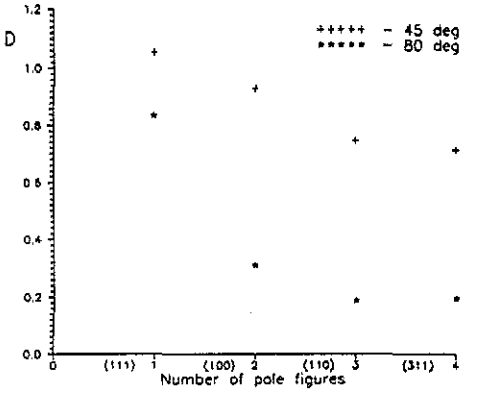

Figure 8. The results of reproduction from one ({111}), two ({111} and {100}), three ({111}, {100} and {110}) and four ({111}, {100}, {110} and {311}) pole figures after 300 iterations. The ranges of pole figures were 45° and 80°.

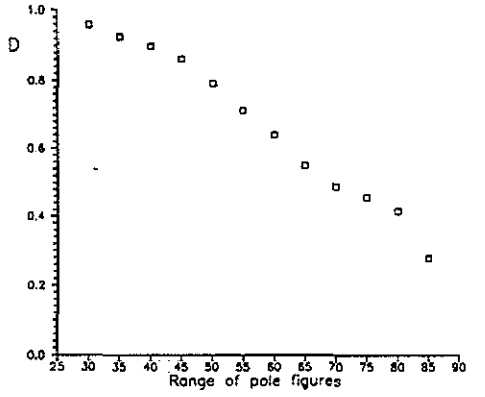

Figure 9. D versus the range of pole figures after 50 iterations.

slope and therefore the program separating the textures requires a larger number of iterations to achieve results of comparable quality.

The dependence of D on the amount of information is shown in figures 8 and 9. As should be expected, the range of pole figures used strongly influences the quality of the results. This follows from the presence of α in equation (10).

The results for different numbers of pole figures are given in figure 9. The fact that for the established range of 80° the convergence for three pole figures is better than for

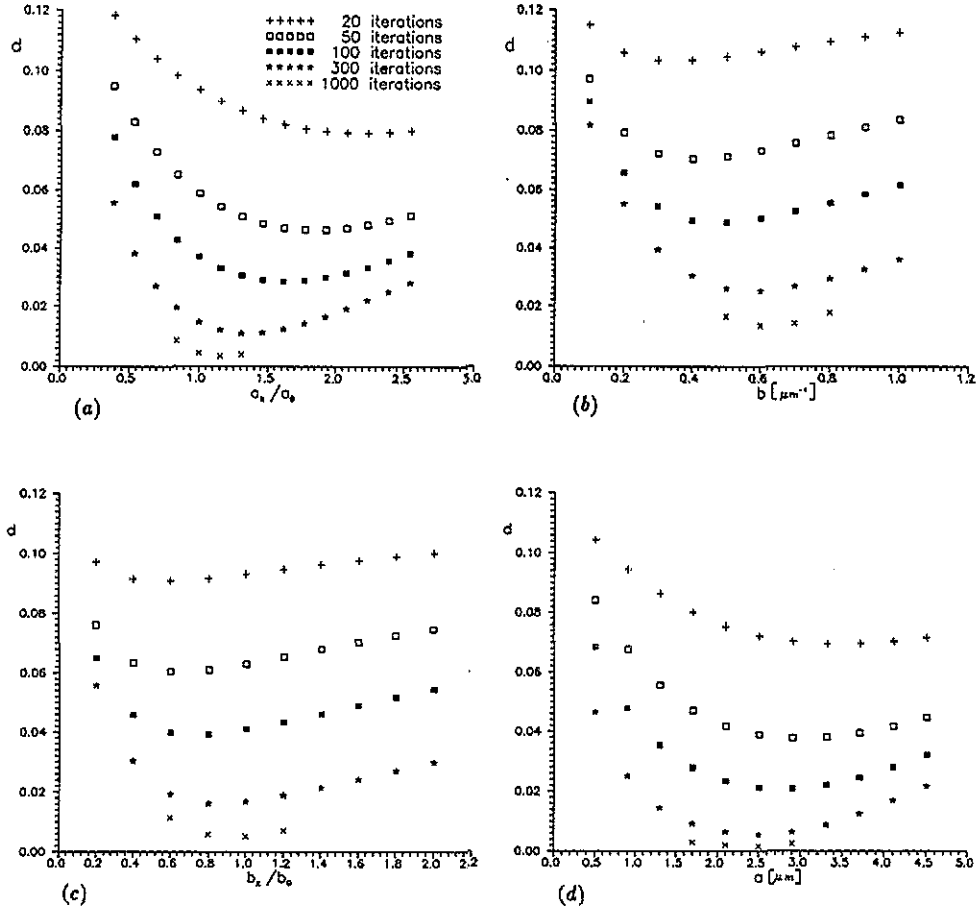

Figure 10. (*a*) Pole figure adjustment versus $\mathcal{A}_x/\mathcal{A}_0$, where $\mathcal{A}_0 = 1.3\ \mu$m corresponds to model textures (9), and $\mathcal{A} = \mathcal{A}_x$ was assumed during reproduction. (*b*) d versus parameter $\mathcal{B}$ of equation (11) for the model texture built according to equation (9) with $\mathcal{A} = \mathcal{A}_0 = 1.3\ \mu$m, and equation (11) assumed during reproduction. (*c*) Pole figure adjustment versus $\mathcal{B}_x/\mathcal{B}_0$, where $\mathcal{B}_0 = 0.5\ \mu\text{m}^{-1}$ corresponds to model textures (11), and $\mathcal{B} = \mathcal{B}_x$ was assumed during reproduction. (*d*) d versus parameter $\mathcal{A}$ of equation (9) for the model texture built according to equation (11) with $\mathcal{B} = \mathcal{B}_0 = 0.5\ \mu\text{m}^{-1}$, and equation (9) assumed during reproduction.

four indicates that the fourth pole figure does not add much more information than already obtained from the three others.

In practice, contrary to the model calculations, the functions ξ_i (describing texture changes with x) will usually be unknown. The question arises of whether from the course of the reproduction process one can guess how texture depends on depth or at least what is the value of the parameters of ξ_i functions ($\mathcal{A}$ in equation (9)). In other words, if the convergence of iteration (as shown by d versus the number of iterations) is the best when the ξ_i-functions used for reproduction are identical with the real functions, i.e. those corresponding to the sample. The results of appropriate tests are given in figure 10(*a*). The minimum of the curve appears near the 'real' value of the parameter $\mathcal{A}$ only after a

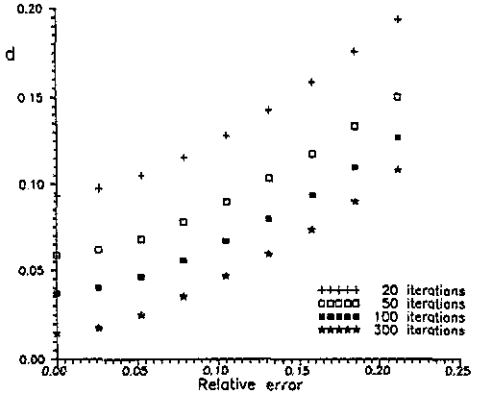

Figure 11. The influence of errors on the adjustment of model and calculated pole figures.

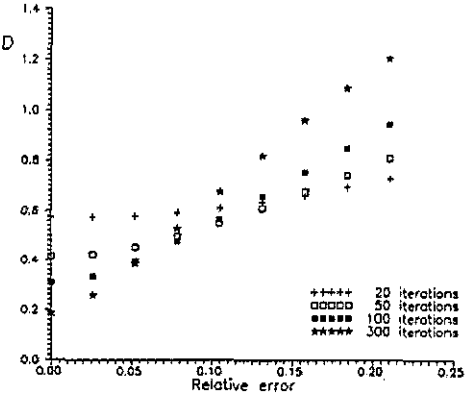

Figure 12. The influence of errors on the calculated texture functions.

very large number of iterations. This in turn, as will be shown, is limited because of experimental errors. Therefore, the possibility of guessing the value of $\mathcal{A}$ is bounded.

The situation is even worse. Let the model be constructed using equation (9), but when reproducing texture functions let us assume that

$$F(g,x) \propto \exp(-\mathfrak{R}x)f^1(g) + [1 - \exp(-\mathfrak{R}x)]f^2(g). \tag{11}$$

The results (D versus $\mathfrak{R}$) for different iteration numbers are shown in figure 10. Here the convergence was better when the reproduction was carried out with the 'true' formula (9) (figure 10(a)) than in case of equation (11) (figure 10(b)). However, unfortunately this is not the case when the role of (9) and (11) are interchanged; the convergence of calculations with an assumed 'untrue' function given by (9) (figure 10(d)) is better than with the proper function given by (11) (figure 10(c)).

All the above tests were carried out using error-free model pole figures. The measured pole figures are within the experimental errors. The question is how the errors influence the reproduction results?

The discussed separation method is based on the incompatibility of pole figures. The pole figures are considered to be compatible if there exists a texture function from which they all can be obtained following equation (4). The limit of the value of d for a large number of iterations is some measure of the incompatibility. It is near zero for compatible pole figures and takes higher values for incompatible pole figures. From a formal viewpoint, incompatibility is equivalent to discrepancy in the system of linear equations which are being solved. On the other hand, the same effect of incompatibility is produced by pole figure errors. Thus the separation method could be error sensitive.

To check this sensitivity, the model pole figures were disturbed in such a way that relative errors had a normal distribution and the error (mean for established α) depended on the radial angle of the pole figure (proportional to $1 + 2 \times 10^{-3} \tan \alpha$). The changes in d and D versus the mean relative error at one 'measurement' point of the pole figure are shown in figures 11 and 12.

When the value of error is high, the increase in the number of iterations does not cause a decrease in D, i.e. does not improve the quality of results. However, even in such a case, although the details are missing, the main maxima can be properly localized.

5. Final remarks

The main advantage of the method presented is that it is much easier to apply than the traditional technique of thinning. It is important also that this is a non-destructive method.

It can be applied to inhomogeneities of different scales; one can investigate thin layers using x-rays or thick samples by neutron diffraction.

A serious limitation is due to the difficulties connected with the determination of the ξ_i-functions. For a small number of iterations it is impossible to draw conclusions about their form from the course of the iteration process. On the other hand, because of experimental errors it is not reasonable to increase the number of iterations above a certain limit.

References

Bauer R E, Mecking H and Lücke K 1977 *Mater. Sci. Eng.* **27** 163
Bunge H J 1982 *Texture Analysis in Material Science* (London: Butterworth)
Choi C S, Prask H J and Trevino S F 1979 *J. Appl. Crystallogr.* **12** 327
Imhof J 1983 *Phys. Status Solidi* b **119** 693
Matthies S 1991 *Proc. 9th Int. Conf. on Textures of Materials* (*Avignon, 1990*) at press
Matthies S, Vinel G and Helming K 1987 *Standard Distributions in Texture Analysis* (Berlin: Akademie)
Morawiec A 1990 *Arch. Metall.* **35** 395
Pawlik K 1986 *Phys. Status Solidi* b **134** 477
Ruer D and Baro R 1977 *J. Appl. Crystallogr.* **10** 458
Truszkowski W, Pospiech J and Pawlick K 1979 *Bull. Pol. Acad. Sci. Tech. Sci.* **27** 171